Pergamon

PII: S0021-8928(97)00118-4

J. Appl. Maths Mechs, Vol. 61, No. 6, pp. 901–915, 1997

0021-8928/97 $24.00+0.00

THE DESIGN OF SYMMETRIC, OPTIMAL SUPERSONIC AND HYPERSONIC FLOW PROFILES FOR ARBITRARY ISOPERIMETRIC CONDITIONS†

A. N. KRAIKO and D. Ye. PUDOVIKOV

Moscow

(*Received* 23 *September* 1996)

A simple and accurate approach to the design of symmetric profiles which are optimal in the supersonic and hypersonic flow with an attached shock is developed. Besides dimensional constraints, the bodies being optimized can satisfy arbitrary isoperimetric conditions. The approach which has been developed uses a modification of the "shock–expansion" method (SEM). The modified shock–expansion method (MSEM), unlike SEM, does not lead to a physically absurd result, that is, to a finite change in the flow parameters when the slope of the contour is solely changed at the leading point of the body. This makes MSEM suitable for solving two-dimensional variational problems in gas dynamics, by reducing any of them to a certain extension of the Lagrange problem for systems which are described by ordinary differential equations. The possibilities of the approach which has been developed are illustrated using examples of profiles which achieve a minimum wave drag coefficient, C_x. Profiles designed using the MSEM are compared with those obtained using the Newtonian model and linear theory and with wedges while the C_x values found for them using the above-mentioned approximate models and MSEM are compared with the results of the numerical integration of Euler's equations.

The number of variational problems in supersonic gas dynamics which have been solved exactly, even in the approximation of an ideal (non-viscous and non-heat conducting) gas, is small. These are plane and axially symmetric problems which allow transfer to a control contour (CC). In the case of profiles from force characteristics which are optimized or specified as isoperimetric conditions, the wave drag, lift-to-drag ratio and moment of the pressure forces are expressed in terms of the CC. Only overall dimensions constraints allow transfer of the geometric conditions onto the CC. Besides the possibility of transferring the conditions of the problem and of the functional being optimized onto the CC, smoothness of the required contours is also necessary in order to use the control contour method (CCM). Unfortunately, almost all optimal contours of bodies with an attached shock wave have internal corner points [1].

There are two ways of overcoming the above constraints. The first proposes the straightforward application of indirect and direct methods of the variational calculus in the approximate equations for the flow of an ideal gas, the Navier–Stokes equations, etc. In such an exact formulation, the indirect methods, while useful in establishing the structure of the optimal configurations, can hardly become the working instrument for solving a wide range of variational problems in gas dynamics. Direct methods and, especially, those in which the conjugate problem of the indirect method is used as an "accelerator" in searching for the optimum are now demonstrating their possibilities in the design of profiles, wings and wing–fuselage combinations which are optimal in transonic flow [2–6].

In supersonic gas dynamics direct methods have not been widely used for two reasons. First, repeated calculation of the flow around a whole family of non-optimal contours is required in these methods. The costs involved in designing optimal plane and axially symmetric bodies in problems which allow of transfer to a CC using direct methods are therefore so much greater than when algorithms based on the CCM are used [7]. Secondly, these costs are increased even further, if the special features of the flows which are being calculated are not taken into account, for example, the calculation of a supersonic flow is carried out using "pseudo-establishment" rather than "a march". On account of this, the supersonic contour of a plane asymmetric nozzle of maximum thrust is designed in [8] using 1 h of CPU time on a Cray Y-MP supercomputer whereas, using the CCM, the same problem can be solved using a PC-AT 486 in less than a minute.

In more complex variational problems in supersonic gas dynamics, which do not allow of transfer to a control contour, it is necessary to precede the analysis of the structure of the optimal configuration by using direct methods in which various approximate models play a special role together with indirect

†*Prikl. Mat. Mekh.* Vol. 61, No. 6, pp. 931–946, 1997.

methods. In supersonic flows, models of this type [9, 10] give the pressure on the body surface as a function of the angle between the normal to this surface and the velocity vector of the free stream. The use of such "local" models reduces problems of the design of optimal plane and axially symmetric bodies in a supersonic flow, to a Lagrange problem for systems which are governed by ordinary differential equations. Local models provide a second method of formulating and solving variational problems in just supersonic gas dynamics as there are no such models in the case of subsonic and transonic flows. The main drawback of local approaches are the restricted ranges of Mach numbers of the free stream M_∞ for which they produce parameters (primarily, the pressure) on the body which are close to the exact values. Thus, the errors in the linear theory rapidly increase as M_∞ and the relative thickness of the body τ increase. The error in Newton's formula increases as both M_∞ and τ decreases. It does, however, remain finite when $M_\infty \to \infty$.

It is impossible to confirm the reliability of local models without falling outside their limits. This is also true when different local models give identical contours. For example, in the problem of the forebody of the profile of minimum wave drag using Newton's formula (when $\tau \leqslant 1$) and according to the linear theory of moderate supersonic velocities, the optimal contour is a straight line (a "wedge") and this applies for any $M_\infty > 1$. In the case of the same problem using Euler's equations, it is true that the optimal contour is also close to a straight line [1, 11–15] but, now, only when $\tau < \tau^m$, where $\tau^m = \tau^m(M_\infty)$ is the thickness of the wedge for which the Mach number behind the shock wave is equal to unity. If the reflection coefficient of the pressure perturbations from the leading shock wave is equal to zero [1, 11–15] and also, when $\tau = \tau^m$ [15], a rectilinear contour also gives the solution in the exact formulation. Another example of the surprising efficiency of Newton's formula is that of the optimal cowls of bodies of revolution with a neck around which flows occur with an attached shock wave. Here, the cowls found using Euler's equations in all of the examples calculated in [16] are better to within just a few per cent with respect to C_x than the cowls designed in the Newtonian approximation and, moreover, for different values of M_∞, including $M_\infty \approx 1.5$, when the values of C_x, found using Newton's formula, differ several fold from the exact values. Up to the present time, there are no other variational problems of the aerodynamics of supersonic flows which have been solved in an exact or almost exact formulation (as in [15, 16]). Apparently, due to this, proper attention has not been given to the efficiency of Newton's method noted above.

In the light of what has been said, it is difficult to overestimate the role of such approximate models which should make it possible to solve with a high accuracy various variational problems of gas dynamics without integrating Euler's equations, etc. Even if they are only applicable to plane configurations in a uniform supersonic flow, they enable one to extend the testing of local models which are not restricted to such narrow limits. The most natural candidate for such a role is the "shock-expansion" method (SEM). Although the first attempt to use this method to design optimal profiles was announced in [17], it is unsuitable for this purpose. The point is that, in SEM, the pressure on a profile around which there is a flow with an attached shock wave depends on the angles of inclination ϑ and ϑ_i of the tangent to its contour at the point being considered and at the leading point i, respectively. Henceforth, the subscripts $i, \ldots$ and ∞ are used to indicate parameters at the point $i, \ldots$ and in the free stream. In variational problems, the dependence of the pressure on the profile on ϑ_i leads to a physically absurd result, that is, to a finite change in C_x when the inclination of the contour is only changed at its leading point. Chapman [17], on realizing the absurdity of this, apparently did not include the term outside the integral, which is proportional to the variation in ϑ_i, in the expression for the increase in C_x when obtaining the necessary optimality conditions. Such a way out of the situation can hardly be regarded as correct.

A modified SEM, MSEM, which is free from the above drawback, is proposed below. It reduces variational problems of the design of profiles in a supersonic flow with an attached leading shock wave to a certain generalized Lagrange problem for system controlled by ordinary differential equations. In spite of this, the boundary-value problem of designing the optimal contour which is obtained in the MSEM is still quite complicated. A further simplification is achieved by sub-dividing its solution into two stages. In the first of these two stages, the "principal" corner point of the required contour is ignored. A corner point is introduced in the second stage using a procedure which is equivalent to, but simpler than, that developed in [15] when designing forebodies of profiles with specified overall dimensions.

1. THE MODIFIED SHOCK-EXPANSION METHOD (MSEM) AND THE FORMULATION OF THE VARIATIONAL PROBLEM

The distribution of the parameters on the contour if, around which there is a supersonic flow, depends solely on the initial segment *iw* of the leading shock wave. In turn, the shape of *iw* is determined by the form of the initial segment *id* of the contour of the body, as shown in Fig. 1(a) and (b). In Fig. 1(a) the segment *if* is smooth while, in Fig. 1(b), there is a corner point at the point *d*. The contour of the body in Fig. 1 is depicted by a heavy line, the shock wave is depicted by a double line and the C^+ and C^- characteristics by thin lines. The x axis of the Cartesian coordinates x, y is directed along the free stream velocity vector $\mathbf{V}_\infty$. The origin of the coordinate system is at the point *i*. If *d* is a corner point of the contour, parameters on the body to the left and right of this point are labelled with the subscripts "d^+" and "d^-", respectively.

In the SEM [13, 18–20], the angle of inclination σ of the shock wave to the x axis is taken as being constant and equal to its inclination at the point *i*, when determining the parameters on *if*. Because of this, the flow behind the shock wave is a simple wave with rectilinear C^+ characteristics, and any flow parameter ω on the body at a point with an inclination ϑ of the tangent to the x axis is a function of ϑ and σ_i

$$\omega = \omega(\vartheta, \sigma_i) \tag{1.1}$$

Of course, the SEM enables one to construct a curvilinear shock wave, but its curvilinearity has no effect on the distribution of the parameters on *if* and in *ifw*. If K_σ and K_ϑ are the curvatures of the shock wave and the stream line behind it, then [18] $K_\sigma = kK_\vartheta$, with a coefficient k which depends on the free-stream parameters and the Mach number M behind the shock wave, that is, on its intensity. While remaining positive everywhere, the coefficient k increases rapidly and only exceeds unity in a small neighbourhood of $M = 1$. Hence, as a rule, the curvature of the body on *id*. In fact, in the case of such bodies, the curvature of the streamlines decreases (in modulus) as they recede from the body. For example, in Fig. 1(b) for finite K_ϑ in the neighbourhood of the point *w*, $K_\vartheta = -\infty$ at the corner point itself. In the case of concave generatrices, the increases in K_ϑ with distance from the body can be compensated by the smallness of the coefficient k. However, in the case of these bodies as well, if this doesn't reach "gradient catastrophes" with the formation of intense secondary shock waves, the angle of inclination of the shock wave *iw* will only vary strongly when ϑ changes strongly on *id*. In direct problems, bodies around which a flow occurs are not characterized by such a "pathology". The SEM therefore produces quite accurate results for these bodies.

In the case of contours which are obtained in variational problems, by virtue of the dependence in (1.1) of the parameters on the body surface on σ_i, it follows from the necessary conditions for optimality that $\vartheta_i \neq \vartheta(0)$ when $\vartheta(x)$ is continuous for $x > 0$. In spite of this, in the SEM, σ_i is determined using

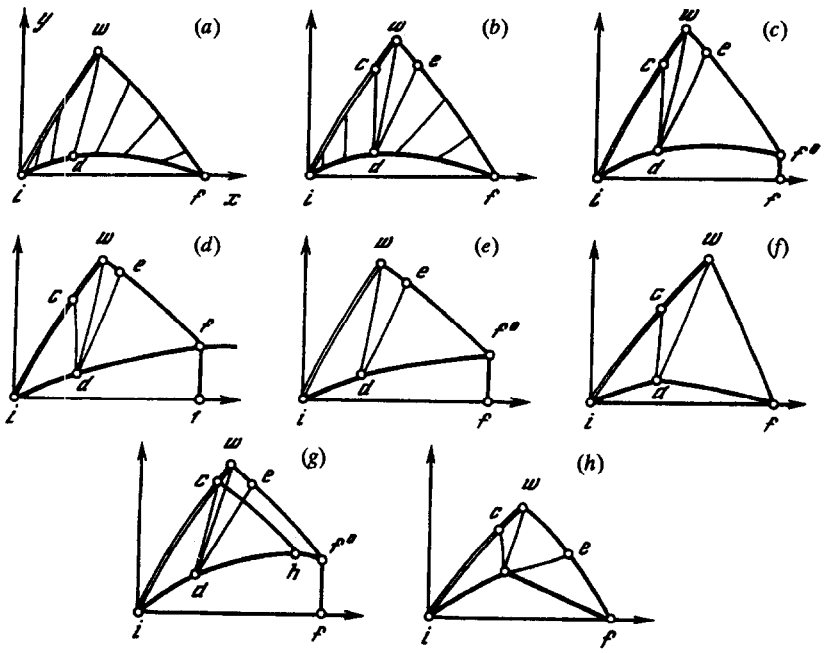

Fig. 1.

ϑ_i rather than using $\vartheta(0)$, although, in the case of such bodies, the value of the angle of inclination of the tangent at the unique point on the body surface does not bear any relation to the slope of the leading shock wave. This flaw in the SEM can be easily eliminated by taking, instead of σ_i, the mean angle of inclination of the shock wave on *iw* or the ratio $\Sigma = x_w/y_w$ associated with it, that is, by using the formula

$$\omega = \omega(\vartheta, \Sigma) \tag{1.2}$$

instead of (1.1).

Unlike the case of σ_i, the shape of the whole of the initial segment of the body *id* is affected by the parameter Σ which occurs in (1.2) and, when there is a convex corner point at point *d*, the part *cdw* of the fan of rarefaction waves which arises in the flow. This effect manifests itself in the following way. As in the SEM, a simple wave with constant parameters on each C^+-characteristics is realized in *ifw*. On account of this, all the flow parameters, in particular, ϑ and the pressure p, are known at the point $x = \zeta$ and $y = \eta$ of intersection of the C^+-characteristics with the shock wave. The local inclination of the shock wave can be found for any of them. Although the emerging arbitrariness can be used to increase the accuracy of the construction of the front shock wave (this was done within the framework of the SEM in [18]) we shall subsequently find its inclination using ϑ. As a result, when account is taken of the rectilinearity of the C^+-characteristics and the differential equation of the shock wave, we obtain

$$L_{11} \equiv \zeta - x + c_1(\vartheta, \Sigma)(y - \eta) = 0, \quad L_{12} \equiv \zeta' - a_1(\vartheta)\eta' = 0$$
$$c_1(\vartheta, \Sigma) = \operatorname{ctg}(\vartheta + \alpha), \quad a_1(\vartheta) = \operatorname{ctg}\sigma \tag{1.3}$$

Here, derivative with respect to the ordinate y of the body are denoted by primes, α is the Mach angle, the dependences of c_1 and a_1 on their arguments are known from the formulae of the simple wave which is realized behind the oblique shock wave with $x_w/y_w = \Sigma$, and y, x and ϑ are the values of the corresponding variables at the point of the contour belonging to the same C^+-characteristic as the point of the shock wave *iw* which is being considered and, subsequently, of the C^--characteristic *wf*. When the point *d* is a corner point, part of the fan may be incident on the shock wave. Then, instead of (1.3)

$$L_{11} \equiv \zeta - x_d + c_1(\vartheta, \Sigma)(y_d - \eta) = 0, \quad L_{12} \equiv \dot{\zeta} - a_1(\vartheta)\dot{\eta} = 0 \tag{1.4}$$

in its section *cw* with the same c_1 and a_1 as in (1.3) but with the replacement in L_{12} of differentiation with respect to y by differentiation with respect to ϑ, which labels the C^+-characteristics of the fan.

If ζ and η are the abscissa and ordinate of the point of the C^--characteristics *wf* then, by analogy with (1.4), its initial and final segments *we* and *ef* are determined by the equations

$$L_{21} \equiv \zeta - x_d + c_1(\vartheta, \Sigma)(y_d - \eta) = 0, \quad L_{22} \equiv \dot{\zeta} - a_2(\vartheta, \Sigma)\dot{\eta} = 0$$
$$L_{21} \equiv \zeta - x + c_1(\vartheta, \Sigma)(y - \eta) = 0, \quad L_{22} \equiv \zeta' - a_2(\vartheta, \Sigma)\eta' = 0$$
$$a_2(\vartheta, \Sigma) = \operatorname{ctg}(\vartheta - \alpha) \tag{1.5}$$

Finally, the tangency condition

$$L \equiv x' - \operatorname{ctg}\vartheta = 0 \tag{1.6}$$

is satisfied on the contour of the body *idf*.

If the contour of the body is specified, the flow around this body is calculated iteratively with the values of Σ found from the preceding approximation. As in the SEM, in the first iteration, $\Sigma = \operatorname{ctg}\sigma_i$. At each iteration, the parameters for the equivalent oblique shock wave, in particular, the pressure $P = p(\Sigma)$, the angle of inclination of the flow $\Theta = \vartheta(\Sigma)$ and the specific entropy $S = s(\Sigma)$ are determined from the exact relations on the shock wave. After this, the equations defining all the flow parameters as functions of ϑ and Σ are written in the form

$$\vartheta - \Theta = \int_P^p \frac{dp}{A}, \quad 2h(p, S) + V^2 = 2H, \quad A = \rho V^2 \operatorname{tg}\alpha \tag{1.7}$$

Here, h and ρ are the specific enthalpy and the density, which are known functions of p and S, V is the modulus of the velocity and H is the total enthalpy. By virtue of (1.7)

$$p_\vartheta \equiv \left(\frac{\partial p}{\partial \vartheta}\right)_\Sigma = A$$

$$p_\Sigma \equiv \left(\frac{\partial p}{\partial \Sigma}\right)_\vartheta = \frac{\Lambda}{A}[A(\Sigma)P' + \Theta'] - \frac{(\ln \Psi)'}{2(\varkappa - 1)A}\int_{\ln P}^{\ln p} K(M)d\ln p \tag{1.8}$$

$$K(M) = \frac{4 + 2(\varkappa - 2)M^2 - (\varkappa - 1)M^4}{\varkappa M^4\sqrt{M^2 - 1}}$$

Here, Λ is the reflection coefficient of pressure perturbations from an equivalent shock wave, $A(\Sigma)$ and Ψ are the values of A from (1.7) and the entropy function $\Psi = \rho p^{-1/\varkappa}$ for it, primes denote differentiation with respect to Σ and the formula for p_Σ is written for a perfect gas with an adiabatic exponent $\varkappa$.

The formulae and Eqs (1.3)–(1.8), after Σ has been replaced by $\sigma_i = \sigma(\vartheta_i)$, enable one to construct the curvilinear shock wave *iw* and the C^--characteristic *wf* in the SEM approximation. In spite of this, the SEM and MSEM are fundamentally different. In the SEM, the shape of the shock wave *iw* and the characteristic *wf* have no effect on the distribution of the parameters in *ifw* and on the contour *if*. In the MSEM, the flow in *ifw* depends on the ratio $\Sigma = x_w/y_w \equiv \zeta_w/\eta_w$, which is found when calculating the flow and, moreover, with a different effect of the initial segment (*id*) and the final segment (*df*) of the contour on Σ. Because of this, in the MSEM, as with Euler's equations, the optimal contour at the point d in the general case will have a corner point. To be sure, in MSEM, due to the replacement of a curvilinear shock wave with a low-shock wave with the mean inclination, it will be unique (at least, in cases when the contour at the corner point is convex) while, within the framework of Euler's equations, the optimal contour has an infinite number of corner points and points of their condensation [1]. This difference, however, is unimportant, since, in the second case, there is no point in taking account of corner points which differ from the large ("principal") corner point [1, 14, 15].† Hence, the MSEM, while not suffering from the flaw which has been noted above in the case of the SEM, predicts such a fine singularity of the optimal contours as the presence in them of an internal corner point.

It has been shown in [10, 17] that a constraint on the length l, which we shall take as the linear scale, plays an important role in variational problems of design of optimal closed bodies. On account of this constraint, the required contour can have segments of a boundary extremum with respect to x in the form of a front face ($x \equiv 0$) or a rear end face ($x \equiv 1$) and even both faces at the same time. The flow around a front face occurs with a detached shock wave and is therefore not considered here. When there is a rear end face $f^\circ f$ (Fig. 1*c*), the pressure p^+ acting on it is assumed to be known and is independent of the shape of the contour if°, around which there is a supersonic flow, and y. In the case of a body which is symmetric about the x axis, the wave drag coefficient C_x is equal to

$$C_x = \int_{y_i=0}^{y_{f^\circ}} p(\vartheta, \Sigma)dy - y_{f^\circ}p^+$$

Here, p and p^+ have been divided by $\rho_\infty V_\infty^2$ while y, like x, has been divided by the length of the body; C_x and subsequently all other integral characteristics are determined for its upper half.

Together with the specification of the length, the body being designed can satisfy N isoperimetric conditions which we shall take to be

$$F^n = \int_{y_i=0}^{y_{f^\circ}} \Phi^n(p, \vartheta, x, y)dy - \int_{y_f=0}^{y_{f^\circ}} \varphi^n(p^+, x, y)dy, \quad n = 1, \ldots, N$$

Here, F^n are known constants, and Φ^n and φ^n are known functions of their arguments; as in the expression for C_x, the second integrals reflect the contribution from a possible rear end face $f^\circ f$ and, in formulating them until the necessary optimality conditions have been obtained, we should not replace x by unity and y_{f° by zero.

†According to [15], for $\Lambda > 0$, when the angle between the tangents at the corner points is particularly small, there can be two corner points with angles similar in value.

2. THE NECESSARY CONDITIONS FOR OPTIMALITY

The isoperimetric conditions are included in the variational problem using a vector of constant Lagrange multipliers μ with components $\mu^1, \ldots, \mu^N$. As a result, in the design of a body which, let us suppose, provides a minimum value of C_x, the latter is replaced by

$$\chi = \int_{y_i=0}^{y_{f^\circ}} \Phi(p, \vartheta, x, y, \mu)dy - \int_{y_f=0}^{y_{f^\circ}} \varphi(p^+, x, y, \mu)dy$$

$$\Phi(p, \vartheta, x, y, \mu) = p + \sum_{n=1}^{N} \mu^n \Phi^n(p, \vartheta, x, y)$$

$$\varphi(p^+, x, y, \mu) = p^+ + \sum_{n=1}^{N} \mu^n \varphi^n(p^+, x, y)$$

For any permissible variation, the variations in C_x and χ are identical. We next put together the Lagrange functional J. For this purpose we add to χ the integrals with respect to y along the contours id_- and d_+f and the integrals with respect to ϑ in the fan of rarefaction waves (only such corner points are subsequently considered) from the left-hand sides of the equations $L_{ik} = 0$ from (1.3)–(1.5) multiplied by variable Lagrange multipliers $\lambda_{ik}(y)$ or $\lambda_{ik}(\vartheta)$ and, also, from the left-hand side of the tangency condition (1.6) multiplied by the variable multiplier $\lambda_0(y)$. For any permissible variation $\delta C_x = \delta J$.

What has been said also holds without change when *if* forms not an isolated body but its forebody (Fig. 1d) with a specified length $x_f = 1$ and ordinate of the terminal point y_f. In this case, the above expression for C_x, with f° replaced by f, differs from the wave drag coefficient by a constant $(p^+ - p_\infty)y_f$, which is unimportant when determining the optimal contour.

On varying the contours *if* shown in Fig. 1(a)–(d), we arrive at the expression

$$\delta C_x = X^d \Delta x_d + Y^d \Delta y_d + [\lambda_{12}(y) - \lambda_{12}(\vartheta)]_{d-}(\Delta\zeta - a_1\Delta\eta)_{c=d-} +$$

$$+[\lambda_{22}(\vartheta) - \lambda_{22}(y)]_{d+}(\Delta\zeta - a_2\Delta\eta)_{e=d+} + X^{f^\circ}\Delta x_{f^\circ} + Y^{f^\circ}\Delta y_{f^\circ} +$$

$$+H^\eta \Delta\eta_w + H^\Sigma \Delta\Sigma + \int_{y_i=0}^{y_d} (A^x\delta x + A^\vartheta\delta\vartheta + A^\zeta\delta\zeta + A^\eta\delta\eta)dy +$$

$$+ \int_{\vartheta_{d-}}^{\vartheta_w} (B^\zeta\delta\zeta + B^\eta\delta\eta)d\vartheta + \int_{\vartheta_w}^{\vartheta_{d+}} (C^\zeta\delta\zeta + C^\eta\delta\eta)d\vartheta +$$

$$+ \int_{y_d}^{y_{f^\circ}} (D^x\delta x + D^\vartheta\delta\vartheta + D^\zeta\delta\zeta + D^\eta\delta\eta)dy - \int_{y_f=0}^{y_{f^\circ}} A^+\delta x dy \qquad (2.1)$$

On the right-hand side of (2.1) the coefficients at the increments Δx_d, Δy_d, etc. and at the variations in the integrands are functions of the coordinates of the contour x and y, of the shock wave $iw - \zeta$ and η and of the characteristic wf or $wf^\circ - \zeta$ and η, of the angle ϑ and other parameters on the contour of the body and at the corner point, if there is one, on the pressure, p^+ and on the quantity $\Sigma = \zeta_w/\eta_w$ as well as constants and the variable Lagrange multipliers. In the case of the forebody when $x_{f^\circ} \equiv x_f = 1$ and $y_{f^\circ} \equiv y_f$ are specified, (2.1) do not contain the last integral and the terms with Δx_{f° and Δy_{f°. The subscripts f° and f are identical for a forebody and for bodies without a rear end face. If the point d is not a corner point, the first four terms and the integrals with respect to ϑ disappear from the right-hand side of (2.1).

In the variation of any (not necessarily) contour shown in Fig. 1(a)–(d) we make the coefficients λ_{ik} at $\delta\eta$ and $\delta\zeta$ in (2.1) equal to zero due to an arbitrary choice of the multipliers. This leads to the system of equations

$$\lambda_{12}'(y) = \lambda_{11}(y), \quad \lambda_{11}(y) = \frac{\lambda_{12}(y)a_1'}{\operatorname{ctg}(\vartheta + \alpha) - \operatorname{ctg}\sigma}, \quad y \in [0, y_d]$$

$$\dot{\lambda}_{12}(\vartheta)=\lambda_{11}(\vartheta),\quad \lambda_{11}(\vartheta)=\frac{\lambda_{12}(\vartheta)\dot{a}_1}{\operatorname{ctg}(\vartheta+\alpha)-\operatorname{ctg}\sigma},\quad \vartheta\in[\vartheta_{d-},\vartheta_w]$$

$$\dot{\lambda}_{22}(\vartheta)=\lambda_{21}(\vartheta),\quad \lambda_{21}(\vartheta)=\frac{\lambda_{22}(\vartheta)\dot{a}_2}{\operatorname{ctg}(\vartheta+\alpha)-\operatorname{ctg}(\vartheta-\alpha)},\quad \vartheta\in[\vartheta_w,\vartheta_{d+}] \tag{2.2}$$

$$\lambda_{22}'(y)=\lambda_{21}(y),\quad \lambda_{21}(y)=\frac{\lambda_{22}(y)a_2'}{\operatorname{ctg}(\vartheta+\alpha)-\operatorname{ctg}(\vartheta-\alpha)},\quad y\in[y_d,y_{f^\circ}]$$

The differential equations, defining λ_{12} and λ_{22} in the four ranges of variation of y and ϑ, allow four conditions. We obtain two of these by equating the coefficients which depend on λ_{12} and λ_{22} in the third and fourth terms of (2.1) to zero, that is, by putting

$$\lambda_{12}(y_d)=\lambda_{12}(\vartheta_{d-}),\quad \lambda_{22}(y_d)=\lambda_{22}(\vartheta_{d+}) \tag{2.3}$$

The derivatives of a_1 and a_2 with respect to ϑ differ. Hence, $\lambda_{11}(y_d)\neq\lambda_{11}(\vartheta_{d-})$ and $\lambda_{21}(y_d)\neq\lambda_{21}(\vartheta_{d+})$ by virtue of (2.3) and (2.2). We obtain the two further conditions which are necessary for determining λ_{ik} by putting $H^\eta=H^\Sigma=0$ in (2.1). This gives

$$[\lambda_{22}a_2-\lambda_{12}a_1+(\lambda_{12}-\lambda_{22})\Sigma]_w=0$$

$$\eta_w(\lambda_{22}-\lambda_{12})_w+\int_{\lambda_{12i}}^{\lambda_{12w}}(\eta-y)c_{1\Sigma}d\lambda_{12}+\int_{\lambda_{22w}}^{\lambda_{22f^\circ}}(\eta-y)c_{1\Sigma}d\lambda_{22}+$$

$$+\int_{\eta_w}^{y_{f^\circ}}\lambda_{22}a_{2\Sigma}d\eta=\varepsilon\equiv\int_{y_i=0}^{y_{f^\circ}}\Phi_p p_\Sigma dy \tag{2.4}$$

$$\Phi_p=\left(\frac{\partial\Phi}{\partial p}\right)_{\vartheta,x,y},\quad \omega_\Sigma=\left(\frac{\partial\omega}{\partial\Sigma}\right)_\vartheta,\quad \omega=p,a_2,c_1$$

Here, as previously, $f^\circ\equiv f$ for forebodies and for bodies without a rear end face. The relation between η and y or ϑ is established from a calculation of the flow about the contour if° within the framework of the MSEM, and the relation between y or ϑ and λ_{12} or λ_{22} is established from the solution of the conjugate problem for the multipliers λ_{ik} which, together with the equations for these multipliers from (2.2), includes conditions (2.3) and (2.4). All the equations and conditions of this conjugate problem are linear in the multipliers λ_{ik} and, apart from the last condition in (2.4), they are homogeneous. The last condition in (2.4) becomes homogeneous if the free-stream parameters and the form of the contour if° are such that $\varepsilon=0$. When $\varepsilon=0$, the solution of the problem for λ_{ik}, which is important later, is trivial, i.e.

$$\lambda_{11}\equiv\lambda_{12}\equiv\lambda_{21}\equiv\lambda_{22}\equiv 0 \tag{2.5}$$

After choosing λ_{ik}, the variations of ϑ in if° enter into expression (2.1) together with the increments of the coordinates of the points d and f°. We employ the arbitrariness in the as yet undetermined multiplier λ_0 in order to make the coefficients at $\delta\vartheta$ vanish. As a result, λ_0 is defined by the finite equations

$$\lambda_0=[(\eta-y)\lambda_{11}c_{1\vartheta}+\lambda_{12}a_{1\vartheta}\eta'-\Phi_\vartheta-\Phi_p p_\vartheta]\sin^2\vartheta,\quad y\in[0,y_d]$$

$$\lambda_0=[(\eta-y)\lambda_{21}c_{1\vartheta}+\lambda_{22}a_{2\vartheta}\eta'-\Phi_\vartheta-\Phi_p p_\vartheta]\sin^2\vartheta,\quad y\in[y_d,y_{f^\circ}] \tag{2.6}$$

$$\Phi_\vartheta=\left(\frac{\partial\Phi}{\partial\vartheta}\right)_{p,x,y},\quad \omega_\vartheta=\left(\frac{\partial\omega}{\partial\vartheta}\right)_\Sigma,\quad \omega=p,a_1,a_2,c_1$$

After this, only terms which are proportional to the increments Δx_d, Δy_d, Δx_{f° and Δy_{f° and integrals of δx in id, df° and $f^\circ f$ remain. When there are N isoperimetric conditions, these increments and variations are not independent. Their independence is achieved by the introduction of N compensating points k_n and the determination of the constant Lagrange multipliers $\mu^1,\ldots,\mu^N$ from the linear system which

is obtained if one puts

$$A^x \equiv \Phi_x - \lambda_0' - \lambda_{11} = 0, \quad D^x \equiv \Phi_x - \lambda_0' - \lambda_{21} = 0 \tag{2.7}$$

at the points k_n in id and df°, respectively.

Satisfying these equalities for the present only at the points k_n enables one, while varying x in the neighbourhood of any point of the contour if at the expense of a simultaneous variation of x in the neighbourhoods of k_n, to preserve the value of all N functionals which have been specified as isoperimetric conditions. Since, on account of the choice of μ, variation of x in the neighbourhoods of the points k_n in no way manifests itself in the expression for δC_x, the δx in id, df° and $f^\circ f$ can now be considered as being independent. Consequently, if the contour idf° provides a minimum of C_x then the first (second) equality of (2.7) must be satisfied over the whole of the interval $id(df^\circ)$.

Similarly, if a corner point ensures a minimum of C_x, then the necessary conditions of optimality, which determine its magnitude and the position of the C^+-characteristic dw in the fan of rarefaction waves, take the form

$$X^d \equiv \lambda_{0d} - \lambda_{0d+} + \lambda_{12d-} - \lambda_{12w} + \lambda_{22w} - \lambda_{22d+} = 0$$

$$Y^d \equiv (\Phi_- - \Phi_+ + \lambda_{0+}x_+' - \lambda_{0-}x_-')_d + \int_{\lambda_{12d-}}^{\lambda_{12w}} c_1 d\lambda_{12} + \int_{\lambda_{22w}}^{\lambda_{22d+}} c_1 d\lambda_{22} = 0 \tag{2.8}$$

In the case of the two-dimensional forebodies, the equations and conditions of the conjugate problem (2.2)–(2.4) and (2.6) for λ_{ik} and λ_0 and the optimality conditions (2.7) and (2.8), at least in principle, enable one to design contours which, by satisfying the N isoperimetric conditions, ensure a minimum value of C_x in the case of supersonic flow around the body with an attached shock wave. In the case of closed bodies of specified length, the optimality conditions at the point f°, which is coincident or is not coincident with f, are obtained in the same way as in [10] and reduce to the inequalities

$$Y^{f^\circ} \equiv (\Phi - \varphi - \lambda_0 \operatorname{ctg}\vartheta - \lambda_{12}a_1)_{f^\circ} \geqslant 0, \quad X^{f^\circ} \equiv \lambda_{0f^\circ} + \lambda_{12f^\circ} \leqslant 0 \tag{2.9}$$

The violation of the first inequality of (2.9) at the point $f^\circ = f$ of a body without an end face is indicative of the need for its introduction. Here, the optimal size of an end face is determined by the same condition with the equality sign. All the values in it (apart from φ) are the limiting values on approaching f° from the left. In the case of a body without an end face, satisfaction of the second inequality of (2.9) indicates that C_x increases as the body length is reduced. For bodies with an end face, the same inequality is the condition that the end face $f^\circ f$ is a segment of a boundary extremum. As in [10], the one further condition that the end face is a segment of a boundary extremum with respect to x takes the form $A^+ = \varphi_x(p^+, 1, y, \mu) \geqslant 0$.

3. TWO-STAGE DESIGN OF THE OPTIMAL CONTOUR

The equations and optimality conditions derived using the MSEM, being incomparably simpler than those to which Euler's equations would lead in similar variational problems, are, nevertheless, still quite complicated. At the same time, experience acquired during the investigation described in [15] suggests that the design of configurations which are close to optimal can be simplified considerably in practice without any loss of quality. This possibility is opened up due to the smallness of ε, on the right-hand side of the second condition from (2.4), and this smallness of ε is a consequence of the smallness of the derivative p_Σ from (1.8). Taking account of this, we can subdivide the design of the optimal contour into two stages. In the first stage, we put $\varepsilon = 0$ which, as will be shown below, gives a contour without a corner point. In the second stage, a corner point is introduced into the simplified version of the approach developed in [15], taking account of the special features, established in [15], of the orientation of the fan of rarefaction waves which arises in a flow around a corner point.

In the first stage, putting $\varepsilon = 0$, we arrive at equalities (2.5) and, then, at a substantial simplification of all the optimality conditions. In the first place, instead of the different equations (2.6) which determine $\lambda_0(y)$ in id and df° and the different optimality conditions from (2.7), now, everywhere on if°

$$\lambda_0 = -(\Phi_\vartheta + \Phi_p p_\vartheta)\sin^2\vartheta, \quad \Phi_x - \lambda_0' = 0 \tag{3.1}$$

Furthermore, it follows from (2.5) and the first condition of (2.8) that the multiplier λ_0 is continuous at the point d and, at the same point, the second condition of (2.8) gives

$$\Phi_{d-} - \Phi_{d+} + \lambda_{0d}(x'_+ - x'_-)_d = 0 \tag{3.2}$$

The first equation from (3.1) holds, in particular, to the left and to the right of point d, while the multiplier λ_0 is continuous at this point. The right-hand side of this equation is therefore also continuous at d. It follows from this and from (3.2) that the generatrix *if*, which corresponds to $\varepsilon = 0$, is smooth. Here, the conditions determining the contour of a closed body without a rear end face (the forebody) and the segments of the contour *if*° and y_{f° of a body with a rear end face as well as the conditions for a closed body at the point f°, which coincides or does not coincide with the point f, do not differ in form from those obtained in [10] in the case of local models. The difference lies in the fact that, in [10], all the parameters are functions only of ϑ, and $p_\vartheta = dp/d\vartheta$. Here, however, all the parameters are functions of ϑ and Σ, while $p_\vartheta = (\partial p/\partial\vartheta)_\Sigma = A$ with $A(p, \Sigma)$ from (1.8) and with Σ, which depend on the shape of *if*°. The smooth contour *if* or its segment *if*° is now determined iteratively. At each iteration, the contour with a rear end face or without it is designed in the same way as in [10], and $\Sigma = x_w/y_w$ is taken from the preceding iteration. The shock wave and the C^--characteristics are constructed and that characteristic which arrives at the point f or f° is found. This characteristic determines the coordinates of the point w and, using it, $\Sigma = x_w/y_w$ for the new iteration.

In the second stage a corner point is introduced into the smooth contour which has been designed. It is not introduced within the framework of the conjugate problem for λ_{ik} and $\varepsilon \neq 0$. We shall therefore refer to the contour which has been designed as "quasi-optimal" in the MSEM approximation. In the same sense, the contour with a corner point from [15] are "quasi-optimal" (within the context of Euler's equations).

The points c and w are coincident in the case of the "quasi-optimal" contours of forebodies designed in [15]. In [15], configurations with a fan of rarefaction waves at the point d correspond to $\Lambda < 0$. When $\Lambda < 0$, the rarefaction waves are reflected from the shock wave as compression waves. It is clear that, in the case of a forebody with $\vartheta_f > 0$, the incidence of compression waves on the end segment of the contour would increase C_x. The flow therefore occurs around the quasi-optimal contours from [15] as shown in Fig. 1(e), giving almost the whole of the reduction in C_x compared with a contour without a corner point.

In the problems being considered, ϑ_f and ϑ_{f° can be of any sign. In accordance with this, the fan is orientated as shown in Fig. 1(e)–(g). If $\vartheta > 0$ at the terminal point of a segment of a contour in a supersonic flow, then the fan is orientated as shown in Fig. 1(e). If $\vartheta < 0$ in a sufficiently large neighbourhood of the same point, then, on the other hand, it is favourable, when $\Lambda < 0$, that it should be reflected from the front shock wave as a whole (Fig. 1f). The "quasi-optimal" decomposition of the fan in the case of small negative ϑ at the terminal point, when the angle ϑ close to its now becomes positive, is carried out according to the scheme in Fig. 1(g) in which $\vartheta_h = 0$. We call the schemes of Fig. 1(f)–(g) "testable" schemes (TC). In order to select the optimal scheme from the TC with the same accuracy as in [15], we proceed as follows.

Suppose that a smooth contour is designed which satisfies all the equations and conditions of the problem and suppose that ϑ_i is the angle of inclination of the tangent at its leading point. We now specify two positive increments of this angle $\Delta\vartheta_{i1}$ and $\Delta\vartheta_{i2}$ and, using the same equations and conditions, we design a further two contours *if* or *if*° in the class of TC but now with a corner point at point d. We ensure that the isoperimetric conditions are satisfied in the case of these contours by the choice of μ.

After the C_x values of the two non-smooth contours from the class of TC have been determined with the same accuracy as in [15], in addition to the $C_x \equiv C_{x0}$ of the smooth contour, we find the coefficients b_1 and b_2 of the quadratic dependence $\Delta C_x \equiv C_x - C_{x0}$ on $\Delta\vartheta_i$

$$\Delta C_x = b_1(1 + b_2\Delta\vartheta_i)\Delta\vartheta_i \tag{3.3}$$

By virtue of this, when $b_1 b_2 > 0$ for the quantity $\Delta\vartheta_i^m$ which gives a minimum of C_x and the ΔC_x^m corresponding to it, we have

$$\Delta\vartheta_i^m = -\frac{1}{2b_2}, \quad \Delta C_x^m = -\frac{b_1 b_2}{4b_2^2} < 0 \tag{3.4}$$

Having described the method of dealing quasi-optimal two-dimensional bodies, we now caution the reader against overestimating the advantages of the MSEM. In particular, in the case of the body shown

in Fig. 1(h) around which there is hypersonic flow, the SEM produces a more correct value for C_x than the MSEM since, for such a body, the segment *id* in which the SEM determines p exactly while the MSEM determines it inexactly provides the main contribution to C_x. On the other hand, for the same reason, in the case of a specified area of the longitudinal cross-section, for example, the quasi-optimal body, as in [10], has a massive afterbody and rear end face which reduce ϑ and p on the surface around which the flow occurs. In the case of such bodies, when determining C_x, it is important to calculate p sufficiently accurately over a large part of the contour *if*° which the MSEM also gives. Of course, in variational problems, the principal advantage of the MSEM lies in eliminating the singular effect on C_x of the angle of inclination of the tangent at the unique point i which is inherent in the SEM. The non-physical inverse effect of the shape of the segment *df*° on the shock wave or, more accurately, on the position of the point w on the shock wave and, consequently, also on the quantity Σ could also be added to the drawbacks of the MSEM. In the complete system of equations and conditions of the conjugate problem and the optimality conditions of Section 2, this effect manifests itself through the multipliers λ_{ik} which appear, for example, in conditions (2.9). However, in the two-stage design of the quasi-optimal contour, this inadequacy satisfactorily disappears. In particular, because of this, the conditions at the point *f*° or *f* become local and exact, agreeing with those obtained using "local variation" [1] in the approximation of Euler's equations.

4. EXAMPLES OF THE DESIGN OF OPTIMAL PROFILES

As an example we will consider closed bodies which give a minimum value of C_x in the case of a specified length and longitudinal cross-section area

$$F = \int_{y_i=0}^{y_{f^\circ}} (1-x)dy - \int_{y_f=0}^{y_{f^\circ}} (1-x)dy$$

In this case, when there is a single constant Lagrange multiplier μ, we have

$$\Phi = p(\vartheta, \Sigma) + \mu(1-x), \quad \varphi = p^+ + \mu(1-x)$$

The equations and conditions which, in this problem, determine the smooth extremal contour *if*° in the first stage and the segments *id* and *df*° of the quasi-optimal extremal contour in the second stage, are identical to those obtained in the case of a local model using a simple wave formula [10]. For a perfect gas, these extrema are obtained by integrating the ordinary differential equation

$$\ddot{y} \equiv \frac{d^2y}{dx^2} = \frac{\mu \operatorname{ctg}\alpha}{2\rho V^2 \cos^4\vartheta}\zeta^{-1}, \quad \zeta = 1 + \frac{4(1-M^2)+(\varkappa+1)M^4}{4\operatorname{ctg}^3\alpha}\operatorname{tg}\vartheta \tag{4.1}$$

in which, by virtue of the necessary conditions for a minimum value of C_x [10],

$$\mu \leqslant 0, \quad \zeta \geqslant 0 \tag{4.2}$$

At the terminal point $f^\circ \neq f$ or $f^\circ = f$ of closed bodies, the conditions

$$(p - p^+ + \rho V^2 \operatorname{tg}\alpha \sin\vartheta\cos\vartheta)_{f^\circ} \geqslant 0, \quad \sin^2\vartheta_{f^\circ} \geqslant 0 \tag{4.3}$$

must be satisfied.

For a body with a rear end face, the first of these conditions (with an equality sign) determines y_{f° while the second condition, together with the first inequality of (4.2), are the conditions for the rear end face to be a segment of a boundary extremum. The difference between the equations and conditions (4.1)–(4.3) and the equations and conditions from [10], which are superficially identical to them, lies in the fact that, in (4.1)–(4.3), all the parameters are functions of ϑ and Σ and not just of ϑ, as in [10].

By virtue of (4.1) and (4.2), the curvature of the optimal contour of closed bodies, as in the local models from [10], is of fixed sign (it is equal to zero in the limit case when $\mu = 0$). In the case of optimal bodies without a rear end face it follows from this that, when $F > 0$, they are convex since, when $\ddot{y} \geqslant 0$, a contour lying above the x axis cannot join the points i and f, which belong to this axis. Incidentally, it can be seen from this that negative values of μ correspond to such bodies. The fact that $\ddot{y}$ has a fixed sign is insufficient for the convexity of optimal bodies with a rear end face. In fact, it is possible to join

Table 1

p^+	0		p_∞			$2p_\infty$		
M_∞	6	12	6	12	18	6	12	18
$C_x^\circ \times 10^2$	1.189	0.785	0.892	0.708	0.663	0.579	0.639	0.638
ΔC_x, %	0.09	0.33	0.11	0.43	0.58	0.16	0.48	0.69
ΔC_{xN}, %			0.51	0.13	0.13	1.44	0.18	0.13
ΔC_{xL}, %	5.25	8.35	2.92	5.65	6.93	0.62	3.13	4.71
ΔC_{xW}, %	29.7	30.3	30.1	31.8	31.7	34.6	32.3	32.3
ΔC_{xD}, %	149	223	233	258	270	412	303	290
$\tau \times 10^3$	148	157	154	158	159	161	160	161
$y_{f^\circ} \times 10^3$	145	156	154	158	159	161	160	161
$x_d \times 10^3$	211	266	217	270	290	222	275	292
$y_d \times 10^4$	513	614	513	616	653	511	618	654
$\vartheta_i \times 10^3$	253	239	245	236	232	238	234	232
$-\Delta\vartheta_d \times 10^4$	90	170	97	158	170	92	150	164
$\vartheta_{f^\circ} \times 10^3$	-110	-67	-2	-9	-16	47	19	43

the point i to the point f° at which $x_{f^\circ} = 1$ and $y_{f^\circ} > 0$ with both a convex contour and a concave contour. Here, the first inequality of (4.2) plays the decisive role. The contour of an optimal forebody can be convex, concave or a straight line segment, depending on the magnitudes of y_f and F.

We will now compare the quasi-optimal contours which are obtained in this problem using the MSEM with the optimal contours which were designed with the same constraints in [10] using the linear theory of two-dimensional supersonic flow and Newton's model.

Typical values of C_x for bodies of minimum drag, designed using the different models, are shown in Table 1. In this table, results obtained for bodies with $F = (\mathrm{tg}30°)/6 = 1/(6\sqrt{3}) = 0.096$ around which there is a flow of a perfect gas with $\varkappa = 1.4$ when $p^+ = 0, p_\infty$ and $2p_\infty$ are collected together. Since F of the upper half of the body is relative to the square of the length, the selected value corresponds to rather thick bodies. So, in the case of a body which is symmetric with respect to $x = 1/2$ and has a parabolic contour, $\vartheta_i = 30°$, $\vartheta_f = -30°$, and the maximum relative thickness $\tau_0 = y(1/2) \approx 0.144$. In the case of bodies with a rear end face, the cross-section of maximum thickness is placed at values of x which are either equal or close to unity and the corresponding value of τ is close to τ_0. Regardless of which model was used for the design, the values of C_x presented in Table 1 were found using the MSEM.

The third row in Table 1 gives C_x, the wave drag coefficient of a quasi-optimal body with a corner point, the contour of which was designed using the second stage of the MSEM. The differences (as a percentage) from this value of the values of C_x, for bodies with a rear end face designed using the first stage of the MSEM (ΔC_x), in the approximation of Newton's model (ΔC_{xN}) and of linear theory (ΔC_{xL}), of a wedge of the same longitudinal area (ΔC_{xW}) and, also, of a pseudo-optimal body without a rear end face (ΔC_{xD}) designed in the linear approximation [21], are shown in the following rows. For the reason explained in [10], optimal Newtonian bodies have only been designed for $p^+ \geqslant p_\infty$. For all bodies $C_x > C_x^\circ$. Nevertheless, ΔC_{xN} turned out to be extremely small for all of the examples which were calculated. While the smallness of ΔC_x is quite natural since, here, as in [15], the corner-point angles are small, the smallness of ΔC_{xN} is surprising, particularly in view of the fact that $C_{xN} < C_x$ in a number of cases. The same is also observed in the case of smaller M_∞. The quantities ΔC_{xL} are also small. In the case of wedges with a rear end face $\Delta C_{xW} \approx 30\%$, while ΔC_{xD} for pseudo-optimal bodies without a rear end face is hundreds of percent.

Several geometrical characteristics of quasi-optimal bodies with a corner point have been collected together in the lower part of Table 1, which correspond to the upper part of the same table. These characteristics are their relative thickness τ, the coordinates x_d, y_d and y_{f°, the angles ϑ_i and ϑ_{f° and the corner-point angle $\Delta\vartheta_d = \vartheta_{d+} - \vartheta_d$. Smooth contours, designed for $M_\infty = 3$, 6, and 12 using the different models, are shown in Fig. 2 for $p^+ = p_\infty$. We have plotted $\eta = y/\tau_0$ along the ordinate. Contours with a rear end face, designed in the MSEM approximation, using linear theory and Newton's model are given by the solid, dashed and dash–dot curves, respectively. The small circles on the solid curves give the positions of the corner points. In addition, a wedge and a symmetric profile with the same area F are shown by the solid lines in the upper part of Fig. 2, corresponding to $M_\infty = 3$.

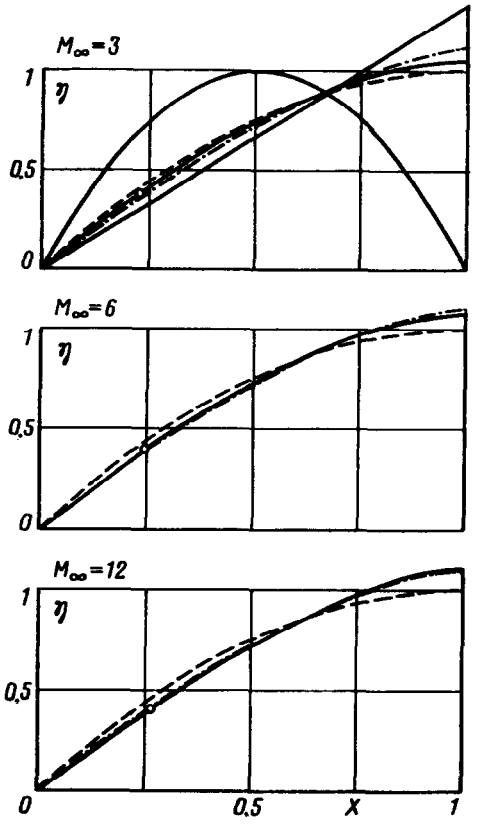

Fig. 2.

The data in Fig. 3 and Table 2 enable one to estimate the effect of the magnitude of p^+ used in the design on the choice of the contours. The smooth contours, designed using the first stage of the MSEM for $M_\infty = 6$ and three values of p^+/p_∞, which are indicated near the curves, are shown in Fig. 3, while the values of C_x and their differences δC_x from the corresponding optimal values are given in Table 2. This table also shows the p^+_{opt} for which the optimal contours were designed and those values of p^+ at which the values of C_x were subsequently calculated. By virtue of this, the values of C_x along the second–fourth columns are the optimal C_x and the differences from these values determine δC_x in the remaining columns of the table. The error in specifying p^+_{opt} by p_∞ increases C_x by not more than 1%.

Figure 4 explains the procedure for the design of quasi-optimal bodies. In this figure, the results of the calculation of $\Delta C_x \equiv C_x^d - C_x^c$ where C_x^c and C_x^d are the values of C_x for the initial (smooth) body and the body with a corner point at the point d, respectively, as a function of $\Delta\vartheta$, determined in an analogous manner, are shown by the small circles. The solid curve is the parabola (3.3) with the coefficients b_1 and b_2 calculated using the values of ΔC_x and $\Delta\vartheta_i$ at the third and fifth points. The closeness of the solid curve to the small circles guarantees the high accuracy of the determination of $\Delta\vartheta_i^m$ and ΔC_x^m using formulae (3.4).

Table 2

p^+	$C_x \times 10^2$			δC_x, %		
	$p^+_{opt}=0$	p_∞	$2p_\infty$	0	p_∞	$2p_\infty$
0	**1.19**	1,20	1.22	**0**	0.9	2.9
p_∞	0.90	**0.89**	0.90	0.9	**0**	0.9
$2p_\infty$	0.61	0.59	**0.58**	5.3	0.9	**0**

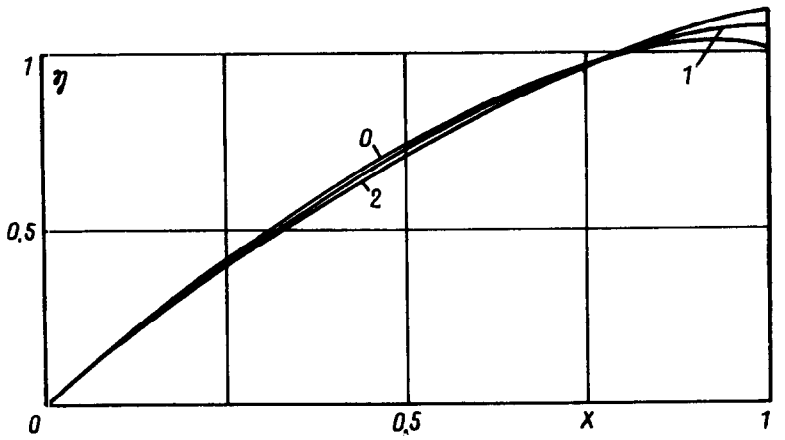

Fig. 3.

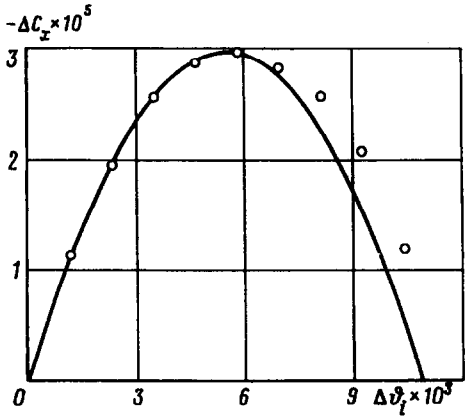

Fig. 4.

Tables 3 and 4 give an idea of the accuracy of the MSEM and other models, in finding C_x, rather than in the design of the optimal contours. Table 3 corresponds to $p^+ = p_\infty$ when the errors in determining p on the contour *if*° are directly reflected in the calculation of C_x. The values of C_x calculated by different methods are presented in this table for various M_∞. Here, C_{xSE}, C_{xLSE} and C_{xNSE} are the values of C_x, calculated using the MSEM, of smooth bodies designed in the MSEM approximation, calculated using linear theory and using Newton's formula. The values of C_x, calculated by integrating Euler's equations using a monotonic second-order marching shock fitting scheme with extrapolation to a zero step size following Richardson, are presented in the third row for smooth bodies designed using the MSEM. A comparison of the second and third rows demonstrates the exceptionally high accuracy of the MSEM. On the other hand, a comparison of the fourth and fifth rows and, also, of the sixth and seventh rows with C_{xL} and C_{xN}, determined using the formulae of linear theory and using Newton's formula, demonstrates the quite acceptable accuracy of the latter. Their efficiency in the design of optimal bodies is quite surprising.

A comparison of the values of C_x of a pseudo-optimal symmetric body without a rear end face, determined using the MSEM (C_{xSE}) and using linear theory (C_{xL}), with the values calculated by integrating Euler's equations (the third row of Table 4) shows some increase in the errors of the MSEM when, as before, the errors in linear theory are completely acceptable. However, for smaller F, for which bodies without a rear end face become optimal, the accuracy of the MSEM is found to be as high as in Table 3. Hence, when used for its direct purpose, that is, for solving problems of optimal design, the MSEM always ensures more than sufficient accuracy.

The modified "shock-expansion" method (MSEM) proposed in this paper enables one to solve problems of the optimal design of spiky two-dimensional bodies in a supersonic or hypersonic flow with

Table 3

M_∞	3	6	12
$C_{xSE} \times 10^3$	13,287	8,932	7,114
$C_x \times 10^3$	13,827	8,928	7,098
$C_{xLSE} \times 10^3$	13,981	9,183	7,481
$C_{xL} \times 10^3$	9,819	4,694	2,322
$C_{xNSE} \times 10^3$	14,012	8,967	7,093
$C_{xN} \times 10^3$	5,345	5,345	5,345

Table 4

M_∞	3	6	12
$C_{xSE} \times 10^3$	44,781	29,666	25,367
$C_x \times 10^3$	44,935	29,476	23,716
$C_{xL} \times 10^3$	39,280	18,779	9,291

attached shock waves, rapidly and with high accuracy. It enables arbitrary isoperimetric conditions to be included in the variational problem and, in the approximation of the integral theory of a boundary layer, enables one to take account of friction and heat fluxes. With an accuracy in determining C_x of optimal bodies which is close to the accuracy of the numerical integration of Euler's equations, the MSEM reduces the problem of design of the optimal contour to a Lagrange problem for systems governed by ordinary differential equations. Despite this considerable simplification, the MSEM, unlike the local models as well as the extremely tedious solution using Euler's equations, gives the principal corner point of the optimal contour. Its occurrence is due to the fact that the reflection coefficient Λ of the pressure perturbations arriving from the body onto the front shock wave, is non-zero. The smallness of Λ enabled us to simplify the solution still further by subdividing the design of the quasi-optimal contours into two stages. A contour without a corner point is designed in the first stage and a corner point is introduced in the second stage using a simple procedure based on the distinctive features of optimal forebodies of specified overall dimensions found in [15].

The rapid and extremely accurate solution of fairly general, though two-dimensional, variational problems in supersonic gas dynamics using the MSEM has enabled us to estimate the possibilities of simpler approximation approaches based on Newton's formula and linear theory as applied to the same problems of optimal design. Comparisons have revealed the surprising efficiency, above all, of Newton's formula, and of linear theory to a somewhat lesser extent, in designing optimal contours, rather than in calculating their C_x.

We wish to thank S. V. Baftalovskii and V. A. Vostretsova for their help.

This research was supported financially by the Russian Foundation for Basic Research (96-01-01825).

REFERENCES

1. KRAIKO, A. N., *Variational Problems of Gas Dynamics*. Nauka, Moscow, 1979.
2. LEE, K. D. and EYI, S., Aerodynamic design via optimization. *J. Aircraft*, 1992, **29**, 6, 1012–1019.
3. REUTHER, J. and JAMESON, A., Aerodynamic shape optimization of wing and wing-body configuration using control theory. AIAA Paper 0123, 1995.
4. JAMESON, A., Optimum aerodynamic design using CFD and control theory. AIAA Paper 1729, 1995.
5. TA'ASAN, S., Trends in aerodynamics design and optimization: A mathematical viewpoint. AIAA Paper 1731, 1995.
6. REUTHER, J., JAMESON, A., FARMER, J., MARTINELLI, L., and SANDERS D., Aerodynamic shape optimization of complex aircraft configurations via an adjoint formulation. AIAA Paper 0094, 1996.
7. BUTOV, V. G., VASENIN, I. M. and SHELUKHA, A. I., The use of non-linear programming method to solve variational problems of gas dynamics. *Prikl. Mat. Mekh.*, 1977, **41**, 1, 59–64.
8. BURGREEN, G. W., BAYSAL, O., and ELESHAKY, M. E., Improving the efficiency of aerodynamic shape optimization. *AIAA Jnl*, 1994, **32**, 1, 69–76.
9. MIELE, A. (Ed.), *Theory of Optimum Aerodynamic Shapes*. Academic Press, New York, 1965.
10. KRAIKO, A. N. and PUDOVIKOV, D. Ye., On the role of a length constraint in the design of minimum drag bodies. *Prikl. Mat. Mekh.*, 1997, **61**, 5, 822–837.

11. CHERNYI, G. G., Supersonic flow around a profile close to a wedge. Tr. Tsentr. Inst. Aviats. Motorostr. im. P. I., Baranova, No. 197, 1950.
12. SHMYGLEVSKII, Yu. D., Supersonic profiles of minimum drag. *Prikl. Mat. Mekh.*, 1958, **22**, 2, 269–273.
13. CHERNYI, G. G., *Gas Flows with High Supersonic Velocity*. Fizmatgiz, Moscow, 1959.
14. SHIPILIN, A. V., Optimum shapes of bodies with attached shock waves. *Izv. Akad. Nauk SSSR. MZhG*, 1966, 4, 9–18.
15. KRAIKO, A. N. and PUDOVIKOV, D. Ye., The design of the optimum contour of the forebody in supersonic flow. *Prikl. Mat. Mekh.*, 1995, **59**, 3, 419–434.
16. KRAIKO, A. N. and SHELOMOVSKII, V. V., Forebodies of solids of revolution with a channel close to bodies of minimum wave drag. *Izv. Akad. Nauk SSSR. MZhG*, 1984, 1, 138–145.
17. CHAPMAN, D. R., Airfoil profiles for minimum pressure drag at supersonic velocities—general analysis with application to linearized supersonic flow. NACA Report 1063, 1952.
18. EGGERS, A. J. Jr., SYVERTSON, C. A. and KRAUS, S., A study of inviscid flow about airfoils at high supersonic speeds. NACA Report 1123, 1953.
19. HAYES, W. D. and PROBSTEIN, R. F., *Hypersonic Flow Theory*. Academic Press, New York, 1959.
20. GUIRAUD, J.-P., *Topics in Hypersonic Flow Theory*. Stanford University, Stanford, CA, 1963.
21. DRUGE, G., Two-dimensional wings of minimum wave drag. In *Theory of Optimum Aerodynamic Shapes* (ed. by A. Miele), Academic Press, New York, 1965.

Translated by E.L.S.